Supplementary Information to
Critical mobility in policy making for epidemic containment

Jesús A. Moreno López,[1] David Mateo,[2] Alberto Hernando,[2] Sandro Meloni,[1,3,4] and José J. Ramasco[1]

[1] *Instituto de Física Interdisciplinar y Sistemas Complejos IFISC (CSIC-UIB), Campus UIB, 07122 Palma de Mallorca, Spain*
[2] *Kido Dynamics SA, Rue du Lion-d'Or 1, 1003 Lausanne, Switzerland*
[3] *Institute for Applied Mathematics Mauro Picone (IAC) CNR, Rome, Italy*
[4] *Centro Studi e Ricerche "Enrico Fermi" (CREF), Rome, Italy*

(Dated: January 22, 2025)

I. MAIN TEXT RESULTS WITH CENSUS LEVEL DATA AND ARTIFICIAL TRIP PATTERNS

In order to check which effects come from the aggregation level of our metapopulation and from the heterogeneity of the mobility data, we developed an iteration of our model that uses census data for home and workplace, in addition to an artificial way to generate extra trips which preserve a power law decay in trip distance distribution but with higher homogeneity and mixing between different zones.

We have employed the population distribution of the city of Madrid together with cell phone data, dividing the province around the city in 293 polygons. These polygons correspond to mobility areas, with all guarantees of preserving privacy, as described by Spain's National Statistics Institute (INE) (`https://www.ine.es/experimental/movilidad/experimental_em4.htm`). In each polygon, we count with an estimation of the resident population based on census. The data is comprised of aggregated trips between residence and workplace areas, having been assigned to every user according to the most common location from 01:00 to 6:00 AM and from 10:00 AM to 08:00 PM respectively. The level of aggregation of this data is higher than the one used in the main text and thus produces sharper transitions in the phase diagram. The INE data only provides home and workplace distributions, thus we must indicate a procedure to generate additional trips.

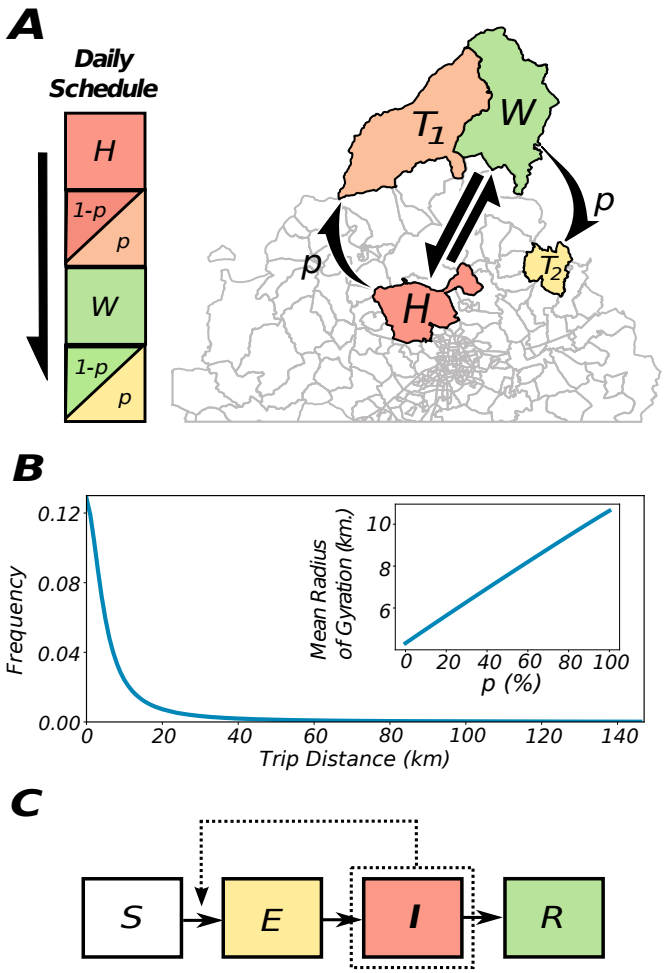

FIG. S1. Summary of model. **A** Sketch of zones where agents can be seen during the day. H and W represent house and workplace respectively, with fixed mobility between them represented in black arrows. T_1 and T_2 represent extra trips that may occur with a probability p, represented with curved white arrows. **B** Trip distance statistics from our model employing equation (1) and relationship between our mobility metric R_g and the trip probability p. **C** Compartmental model. Transition rates and other parameters are identical to the main text. The compartments consist of the following states: susceptible S, exposed E, infected I and recovered R.

In the following additional results, the distance to each destination of Trip 1 (T_1) and Trip 2 (T_2) is sampled from a discrete version of a Cauchy distribution (Fig. S1B):

$$P(d) = \frac{1}{Z\left[1 + \left(\frac{d}{\gamma}\right)^2\right]}, \tag{1}$$

where Z is a normalization constant and $\gamma = 5km$ so that 99% of the distances sampled fall under 147 km, the maximum distance that can be traveled within the Madrid region. Due to the social nature of mobility, once the distance d is determined, the destination of that trip will be sampled from the locations at distance d to the origin, using their population as weights for the sampling. This introduces a high level of homogeneity and mixing in the population.

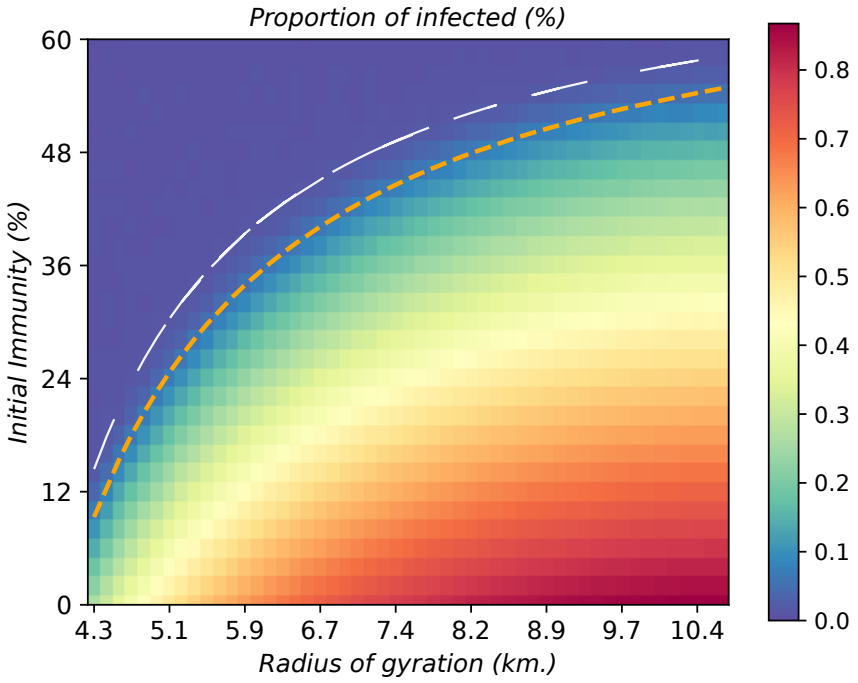

FIG. S2. Epidemic size, i.e., the fraction of infected individuals at the end of the simulation, as a function of the population mobility R_g and the initial immunity levels for infectivity $\beta = 0.1$. The dashed white line shows eq. (2) performed to points with epidemic size between 1.3% and 2.5%, used to estimate the critical mobility threshold $R_{g,c}$ based on immunity. Equivalently, the dashed orange line is another fit performed to mark the boundary below which mobility induces at least a 5% outbreak.

This method produces an abrupt transition between the stale and outbreak phases which can be artificially set at a final proportion of infected population between 1.3% and 2.5%. The observed transition allows us to define a series of boundary points in which to perform a fit and obtain a single estimation for $R_{g,c}$, the critical mobility threshold estimated for each level of immunity in the population. We fit $R_{g,c}$ with:

$$R_{g,c}(km) \approx 2.56 - \frac{1.03}{x - 0.71} \tag{2}$$

where x is the fraction of immune individuals in the population. This simple equation allows us to interpolate the critical curve as a function of the immunity in the population. Below, we present the analogous figures to the main text using this method and data.

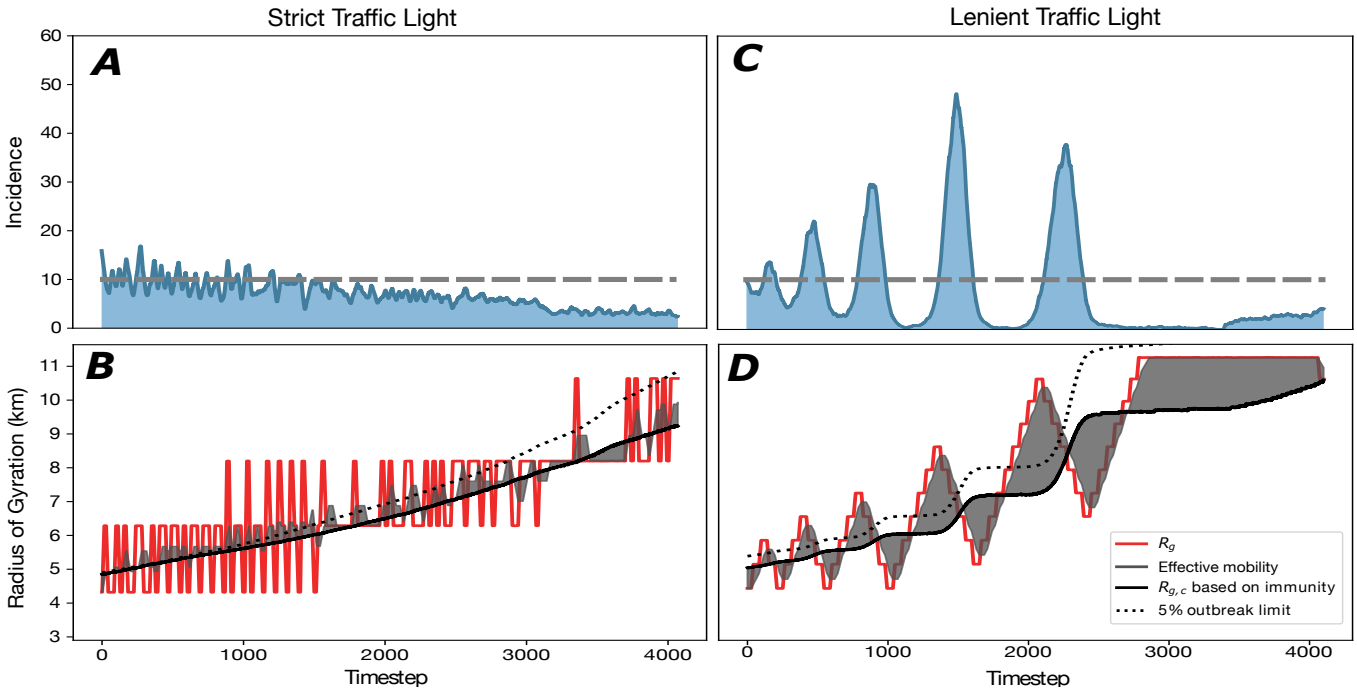

FIG. S3. Examples of incidence threshold-based interventions for infectivity $\beta = 0.1$. The first uncontrollable epidemic wave is removed due to being completely uncoupled from the dynamics the different interventions induce. (**A** and **B**) Incidence per 100 000 inhabitants and mobility curves throughout a realisation of strict traffic light interventions without vaccination. Mobility is adjusted every $T_r = 30$ timesteps and adopts the traffic light values stated in the main text immediately. The grey dashed line in **A** and **C** represents an incidence rate of 10 daily cases per 100 000 individuals. (**C** and **D**) Epidemic and mobility curves throughout a realisation of lenient traffic light interventions without vaccination. Mobility aims to adopt the traffic light values stated in the main text progressively, in changes of $\Delta p = 10\%$ revised every $T_r = 60$ timesteps. **B** and **D** include the 5% outbreak mobility limit plus a 90 timestep moving average of R_g as a measure of an effective mobility.

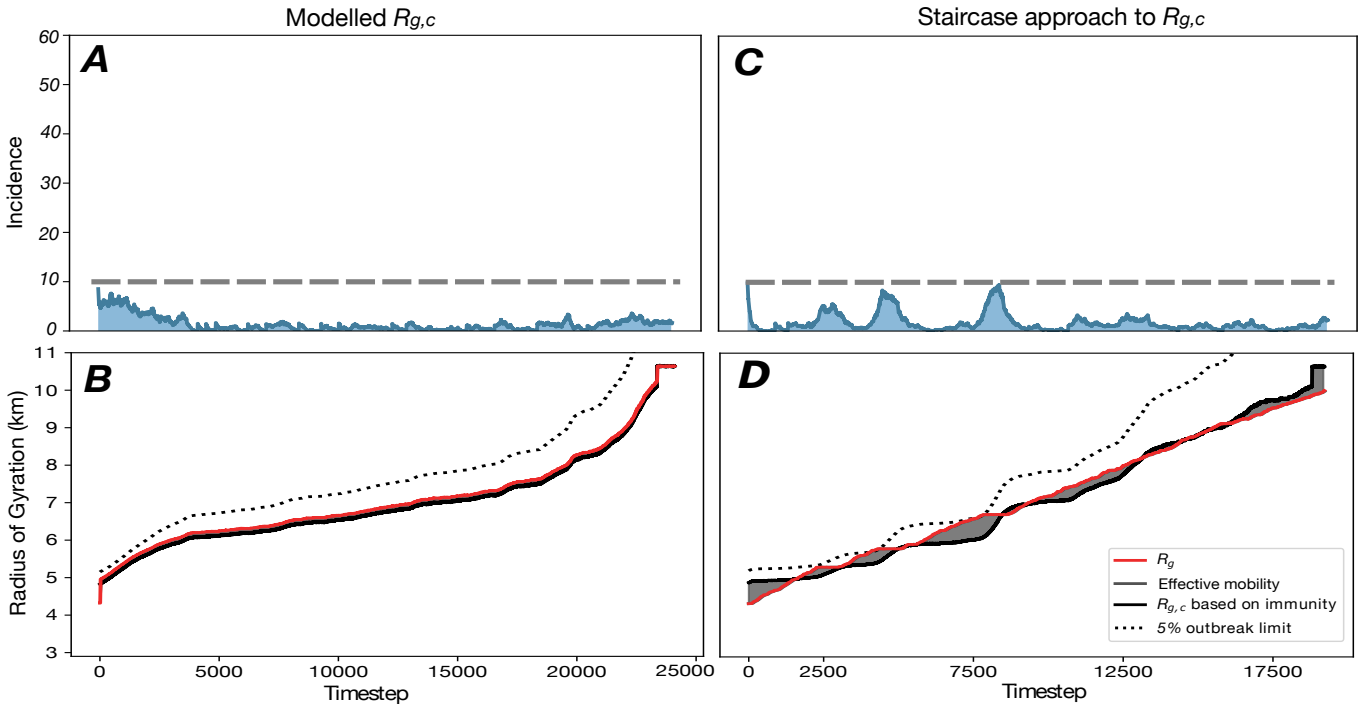

FIG. S4. Examples of R_g-based interventions for infectivity $\beta = 0.1$. The first uncontrollable epidemic wave is removed due to being completely uncoupled from the dynamics the different interventions induce. (**A** and **B**) Incidence per 100 000 inhab. and mobility curves throughout a realisation of an R_g-based intervention with theoretically estimated $R_{g,c}$ without vaccination. Mobility is adjusted every $T_r = 30$ timesteps following the method described in the main text, i.e., adjusted to match $R_{g,c}$. (**C** and **D**) Epidemic and mobility curves throughout a realisation of staircase interventions without vaccination. The mobility parameter p is forced to be monotonically increasing through time in steps of $\Delta p = 0.3\%$ every $T_r = 30$ timesteps. The grey dashed line in **A** and **C** represents an incidence rate of 10 daily cases per 100 000 individuals. **B** and **D** include the 5% outbreak mobility limit plus a 90 timestep moving average of R_g as a measure of an effective mobility. The 90 t.s. average completely overlaps R_g as changes are too slow for them to be distinguishable.

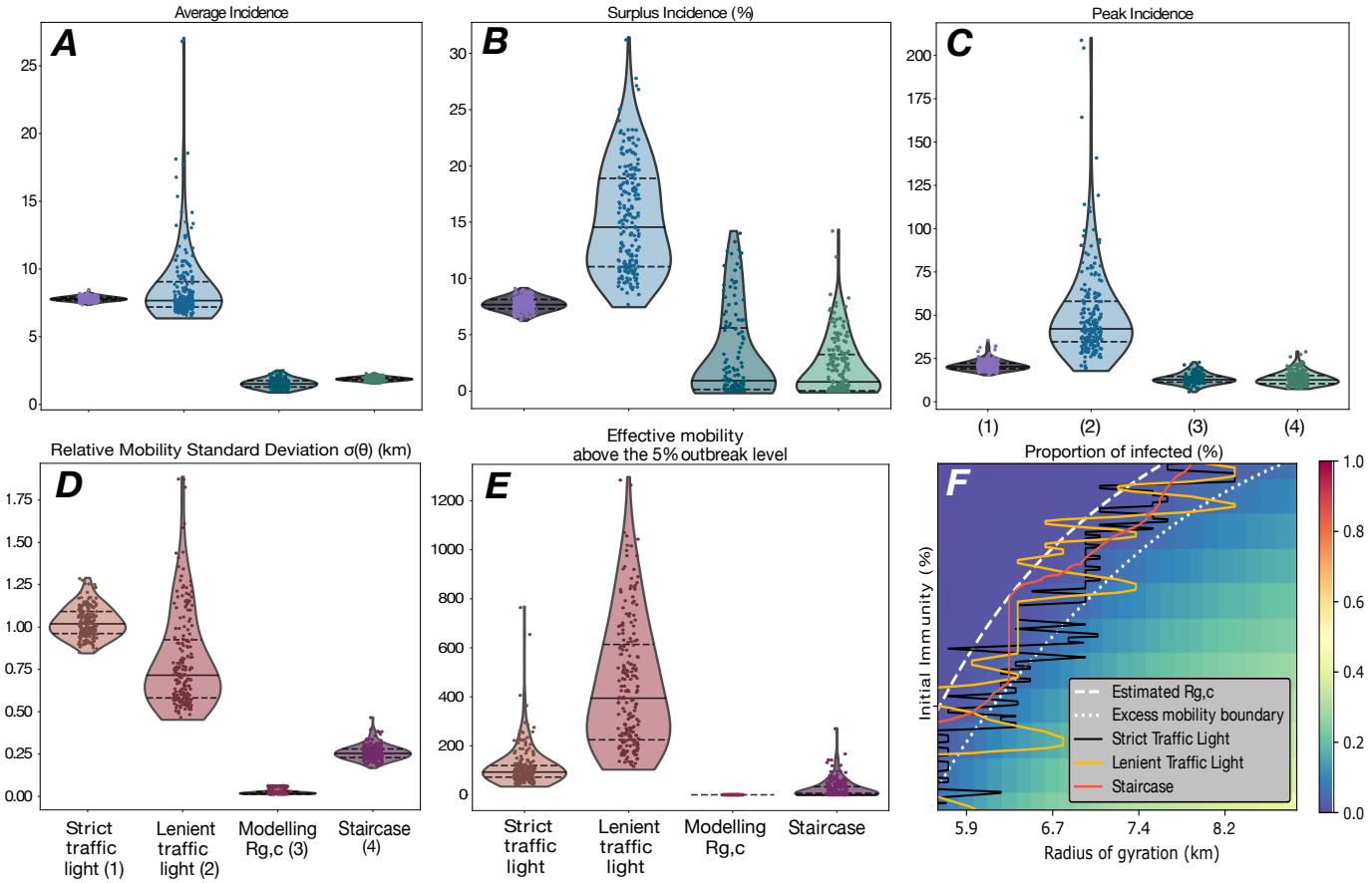

FIG. S5. Violin and strip plots for statistics of the different metrics and interventions tested. The parameters of each intervention are detailed in figures S3 and S4. Violin plots include lines to mark median and quartiles of the distribution. The first epidemic wave happens with $p = 0$ and thus is uncontrollable. Therefore it is excluded when computing the present statistics to avoid dilution of the results produced in the regions where interventions are acting. The number of simulations for each intervention is 200. **A** Average Incidence per 100 000 inhab. **B** Surplus Incidence as a percentage of the total population. **C** Distribution of Peak Incidences by intervention type. **D** Deviation of mobility from the optimum, characterised as the standard deviation of the relative mobility $\Theta(t) := R_g(t) - R_{g,c}(t)$. **E** Cumulative effective mobility (moving average of R_g with a 90t.s. window) above the 5% outbreak mobility level. **F** Example trajectories in the phase diagram of Fig. S2 for interventions shown in Fig. S3 and S4.

II. COMPLEX COVID-19 MODEL [29]

To check whether our claims on the critical transition in the immunity-mobility diagram hold for other more complex epidemiological models, we produced other immunity-mobility diagrams with a complex COVID-19 model from [29], increasing the detail even further by excluding severely infected, hospitalised, ICU and deceased individuals from participating in transmission and epidemiological contacts (figure S6). We can observe how the size and duration of the first epidemic wave will vary between 2 values of β for the same model due to the shift of position of the critical mobility boundary curve (red band in figure S6 C).

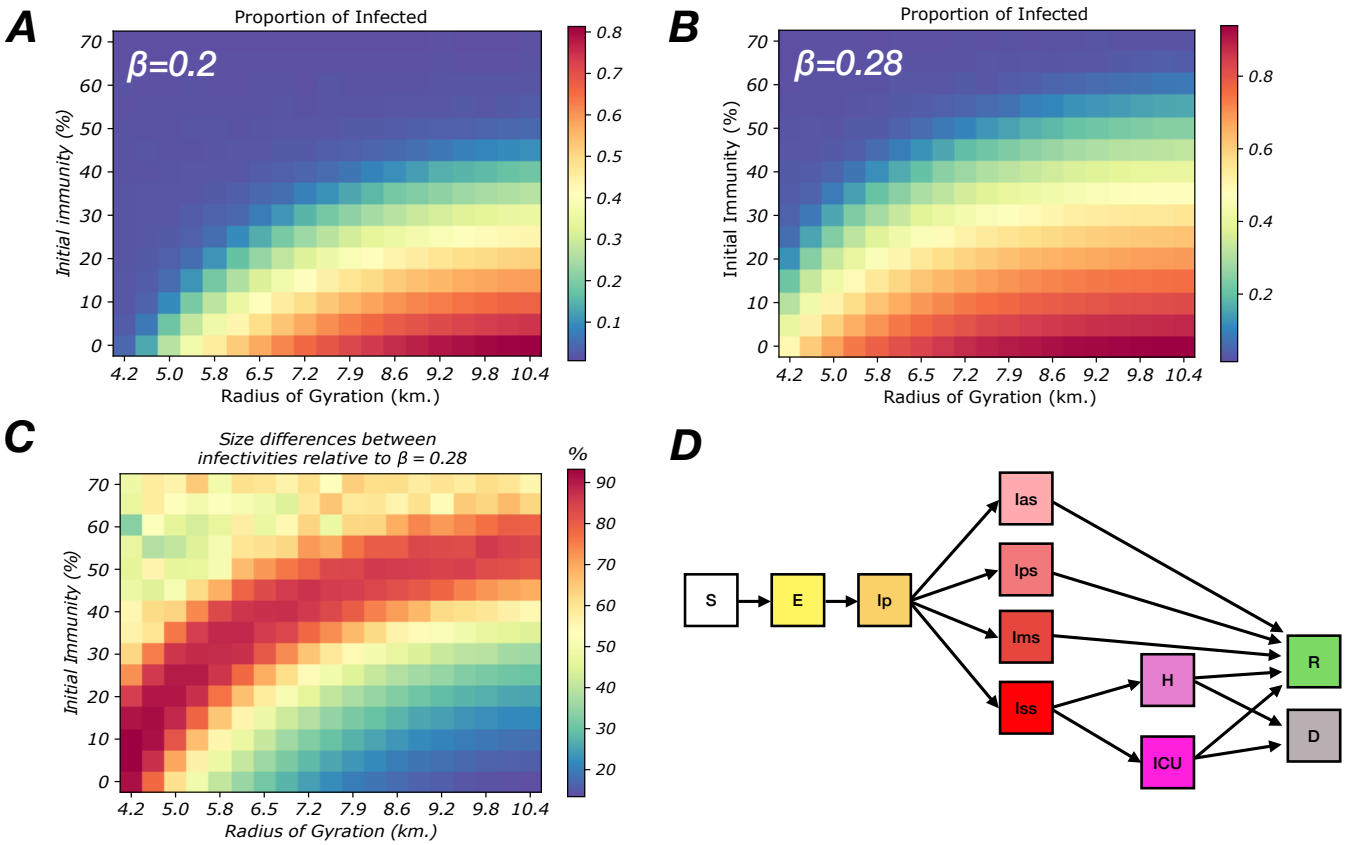

FIG. S6. **A**. Epidemic size, i.e., the fraction of infected individuals at the end of the simulation, as a function of the population mobility R_g and the initial immunity levels for infectivity $\beta = 0.2$ in a complex COVID-19 compartmental model [29]. **B**. Epidemic size as a function of the population mobility R_g and the initial immunity levels for infectivity $\beta = 0.28$ in a complex COVID-19 compartmental model [29]. **C**. Size differences between infectivities $\beta = 0.2$ and $\beta = 0.28$ relative to $\beta = 0.28$ for initial immunity levels and population mobility R_g. **D**. Complex compartmental model inspired by [29] used in the previous panels. The compartments correspond to: S, susceptible; E, exposed; I_p, infectious in the prodromic phase; I_a, asymptomatic infectious; I_{ps}, paucysymptomatic infectious; I_{ms}, mild symptoms; I_{ss}, severe symptoms; H, cases admitted into hospitals (excluding intensive care); ICU, severe cases in ICU; R, recovered; D, deceased. Transition rates can be found in table SI.

Transition	Rate
$E \to I_p$	$(3.7t.s.)^{-1}$
$I_p \to I_{as}$	$0.35 * (1.5t.s.)^{-1}$
$I_p \to I_{ps}$	$0.65 * 0.2 * (1.5t.s.)^{-1}$
$I_p \to I_{ms}$	$0.65 * 0.7 * (1.5t.s.)^{-1}$
$I_p \to I_{ss}$	$0.65 * 0.1 * (1.5t.s.)^{-1}$
$I_{as} \to R$	$(2.3t.s.)^{-1}$
$I_{ps} \to R$	$(2.3t.s.)^{-1}$
$I_{ms} \to R$	$(2.3t.s.)^{-1}$
$I_{ss} \to H$	$0.76 * (2.3t.s.)^{-1}$
$I_{ss} \to ICU$	$0.24 * (2.3t.s.)^{-1}$
$H \to R$	$0.083(t.s.)^{-1}$
$H \to D$	$0.0031(t.s.)^{-1}$
$ICU \to R$	$0.76 * (21.1t.s.)^{-1}$
$ICU \to D$	$0.24 * (21.1t.s.)^{-1}$

TABLE SI. Table with rates for the compartmental model in figure S6D inspired by [29]

III. EVOLUTION OF THE CRITICAL BOUNDARIES

In order to demonstrate the importance of the infectivity when it comes to the effectiveness of measures, we have produced figure S7, showing the shift. This illustrates the logic and importance behind considering a reasonable range of infectivities.

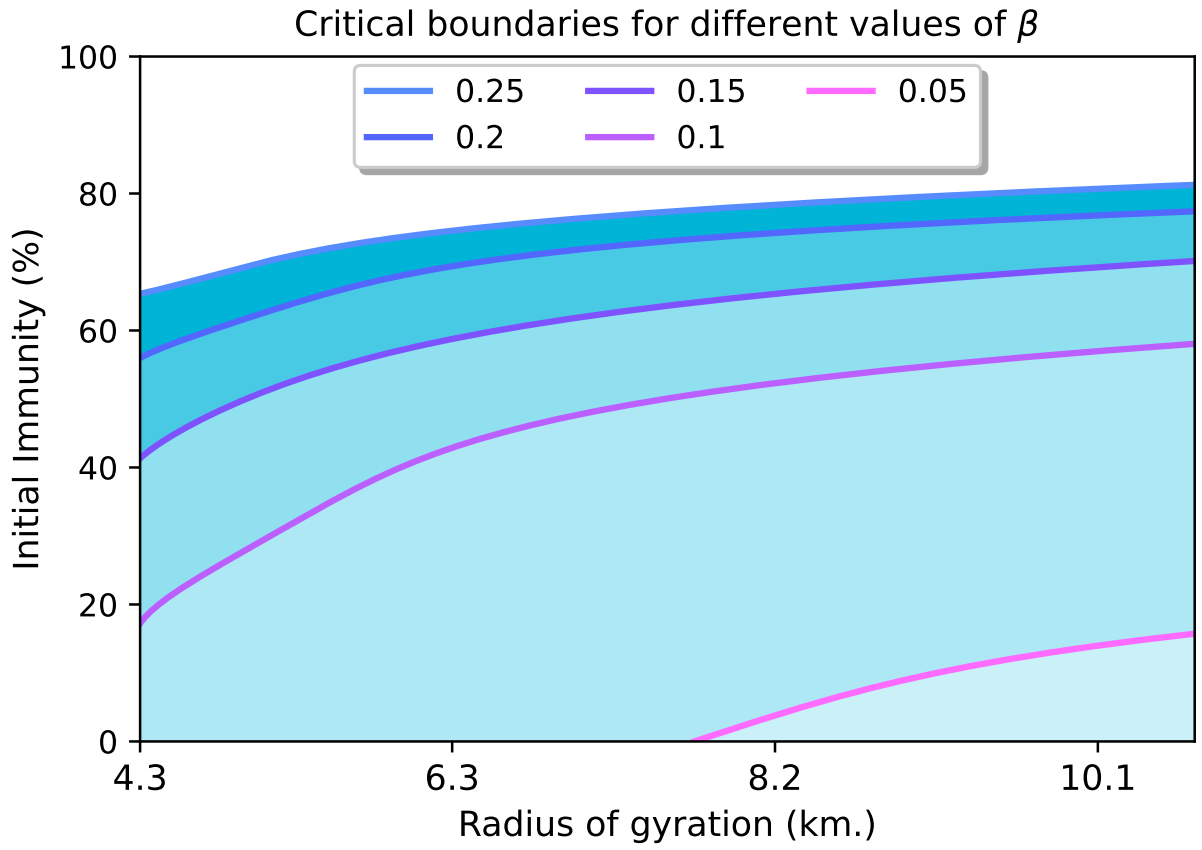

FIG. S7. Evolution with infectivity β of the critical boundary separating the regions of major epidemic outbreaks from stale reactions to seeding in our model.

IV. EFFECTS OF VACCINATION

Vaccination introduces immune individuals each timestep, thus reducing the available population for infection and limiting the total length of the simulations. In order to check if vaccination radically changes our results, figure S8 compares our epidemic metrics without vaccination to a rate of 10 and 50 vaccinations per timestep. Assuming a herd immunity of around 60% (Fig. 2), this bounds our total simulation time to $60 * 10^3$ t.s. for 10 vacc./t.s. and $12 * 10^3$ t.s. for 50 vacc./t.s.. Figure S3 shows no qualitative change in epidemic metrics between interventions, except the expected shifting of distributions towards weaker outbreaks in the case of a very high vaccination rate, supporting our claims that vaccination qualitatively doesn't affect the results, it only shortens the simulation window.

V. STABILITY OF THE TRAFFIC LIGHT SYSTEM

In our model, the traffic light system has divided the possible mobility spectrum into 4 equally-spaced as a proxy for epidemic containment. Being these values arbitrarily chosen for our model, an exploration of different values can be performed to check the error induced by this proxy. We replicate the strict traffic light intervention, except we now skew the CI_{14} thresholds, making the system default to lower values of p (figure S4, skew 1). On the other hand, values can be skewed to default the system to higher values of p (figure S4, skew 2). Skewing the values makes it harder for the system to approximate the mobility to it's critical level at each given time and thus incidence metrics result in higher values than before , specially when the system defaults to higher p values (skew 2). Having this in mind, the difference to our proxy isn't big enough to be worried about our assumption of values for the traffic light system.

To see the stability of this intervention style drawn to the limit, we can reduce it to 2 mobility states with a single threshold: $p = 0$ for $CI_{14} \geq 150$ and $p = 1$ for $CI_{14} < 150$. In figure S5 we explore how the system reacts to this intervention with different revision intervals T_r. With a small enough T_r (T_r $7 - 15$ t.s.) the system seems to stabilise into a low oscillatory regime, although not with incidences as low as when using a traffic light system with a finer spectra of states.

VI. DEGREES OF LENIENCY

When introducing an example of leniency in the application of the traffic light intervention, we chose to revise the mobility every $T_r = 60$ t.s. and only change the mobility parameter p by $\Delta p = 10\%$ when mobility is revised. We know explore both Δp and T_r starting from the baseline for strict traffic light interventions, which would be $\Delta p = 100\%$ and $T_r = 30$ t.s..

From figure S6A we can observe how traffic light systems seem to be robust until $T_r > 30$ t.s., at which point the timescale at which contacts, infections and symptoms onset occur is much smaller than the revision interval and the system cannot react in time, producing oscillations and high incidence rates. Figure S6B shows that failing to adjust mobility to the traffic light system by using changes in the parameter smaller than $\Delta p = 0.25$ result in a substantial increase in incidences and oscillations.

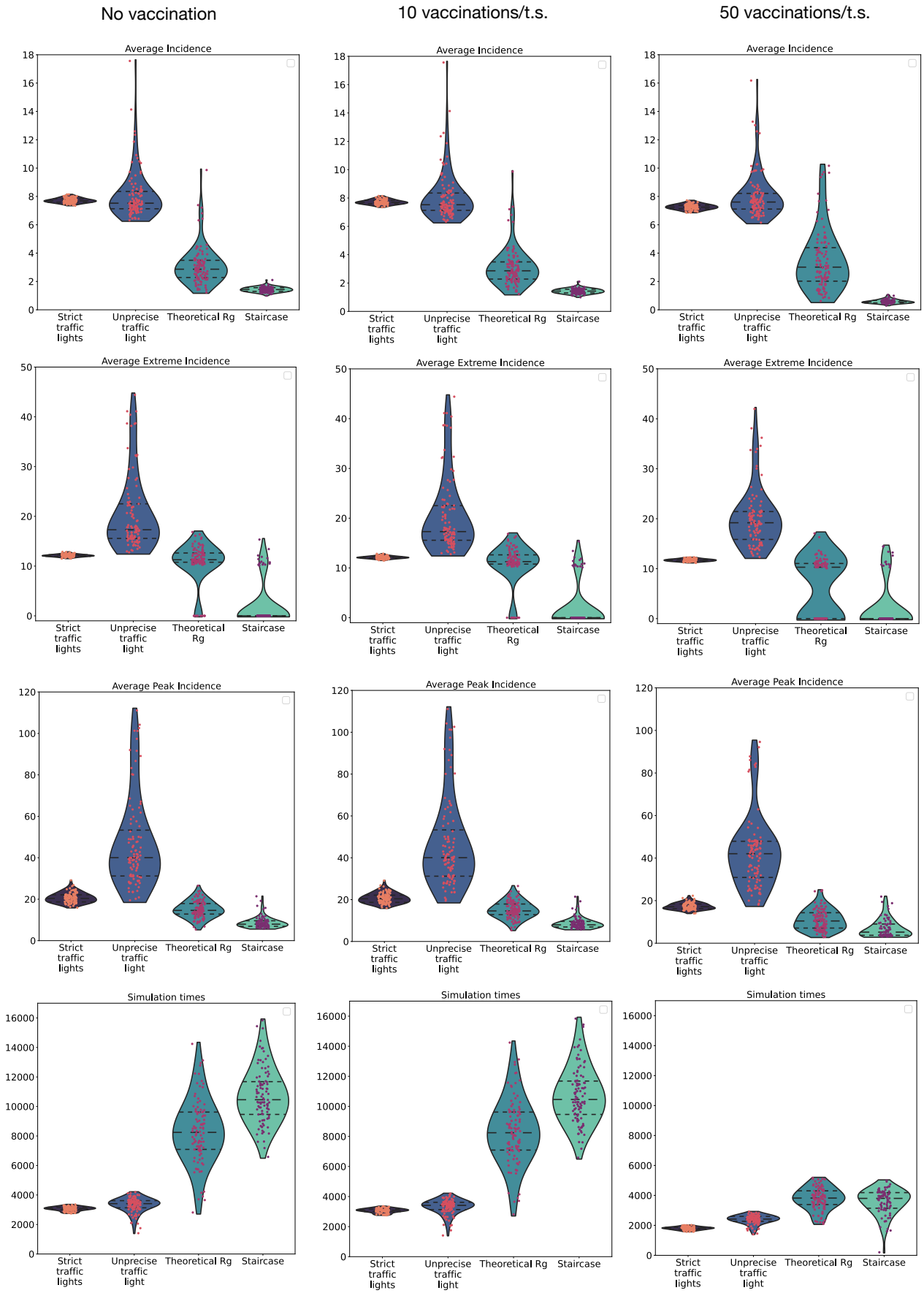

FIG. S8. Epidemic metrics and simulation times for no vaccination, a vaccination of 10 individuals per timestep and a vaccination of 50 individuals per timestep. The interventions used to generate these statistics are the same as the ones described in the main text.

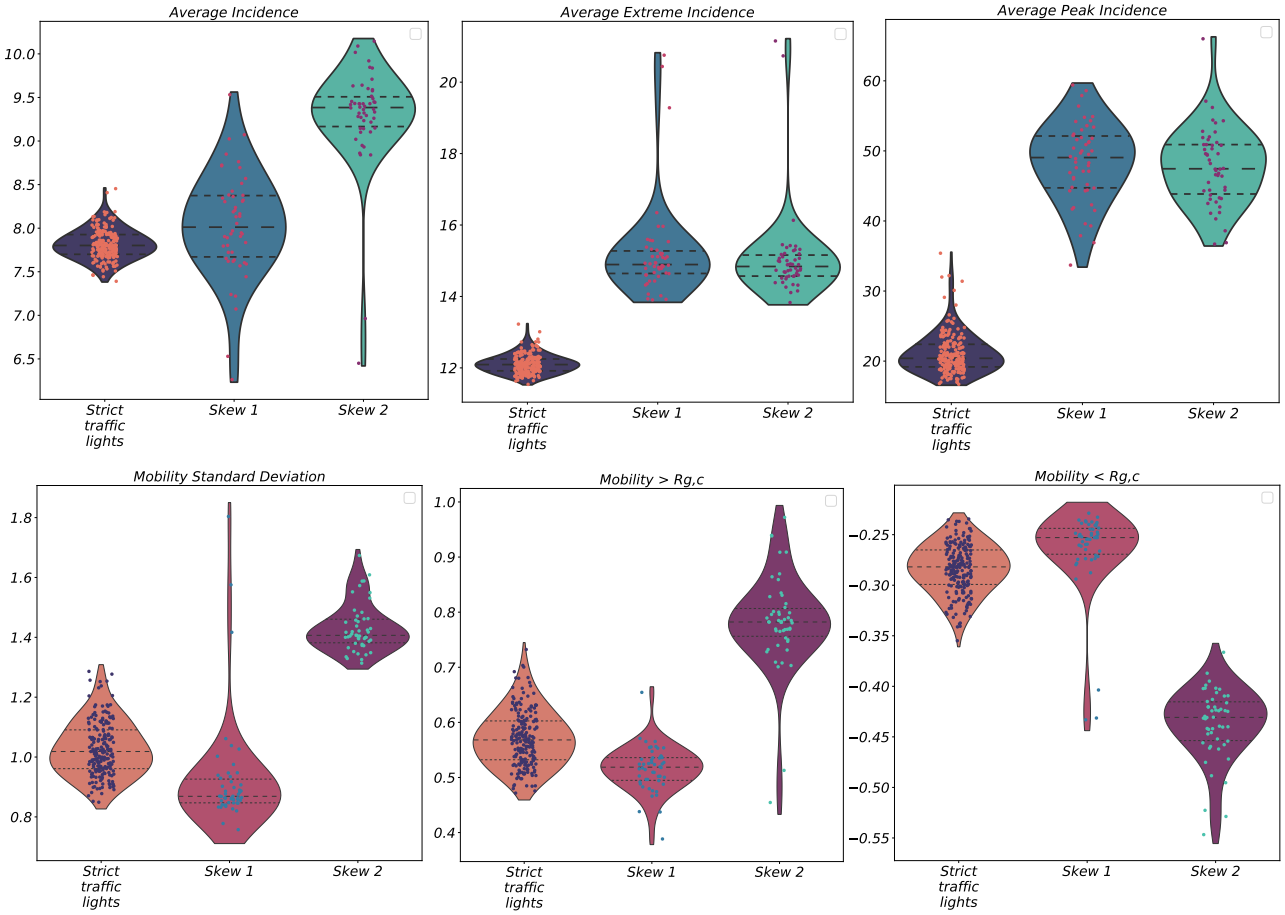

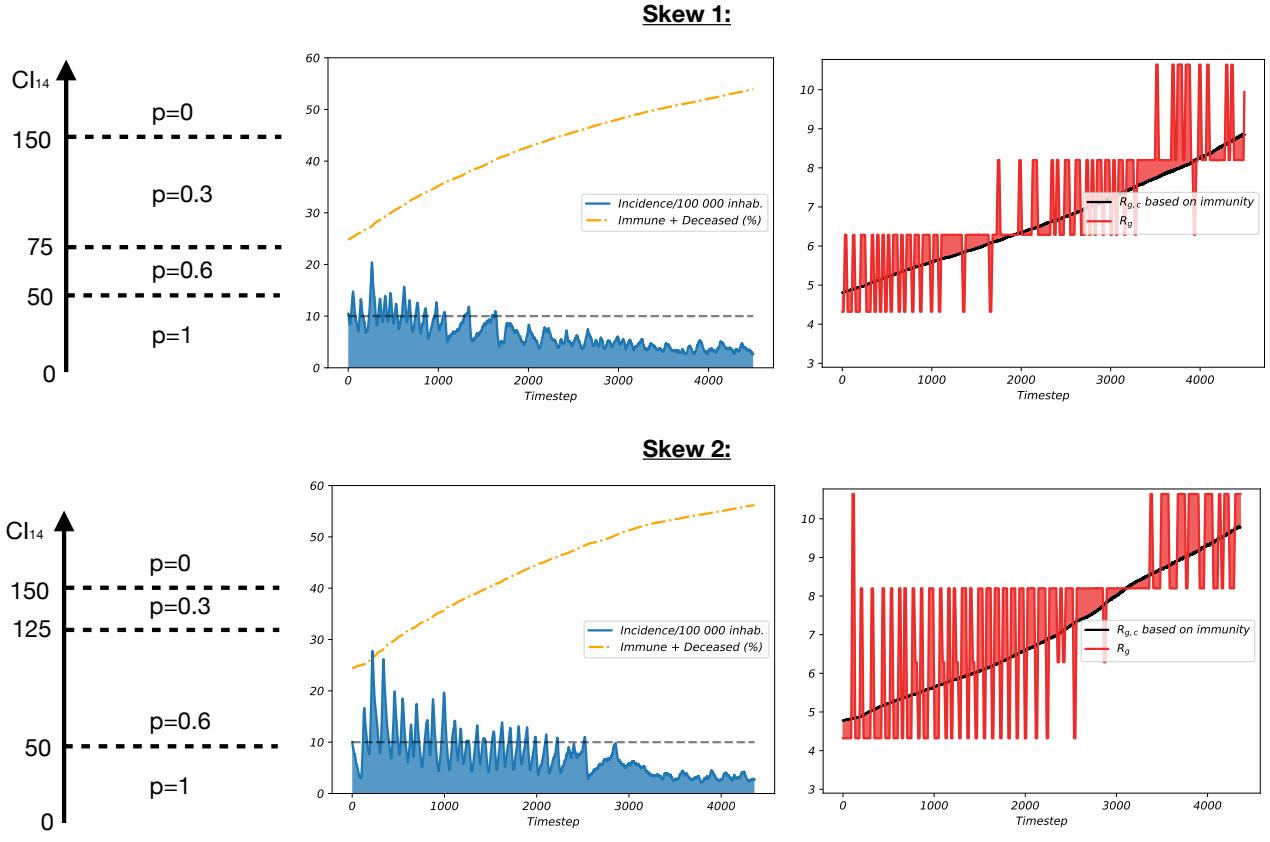

FIG. S9. Epidemic and mobility examples and statistics corresponding to the strict traffic light intervention described in the main text and a skewing of the CI_{14} thresholds used in our strict traffic light intervention. $T_r = 30$ t.s.

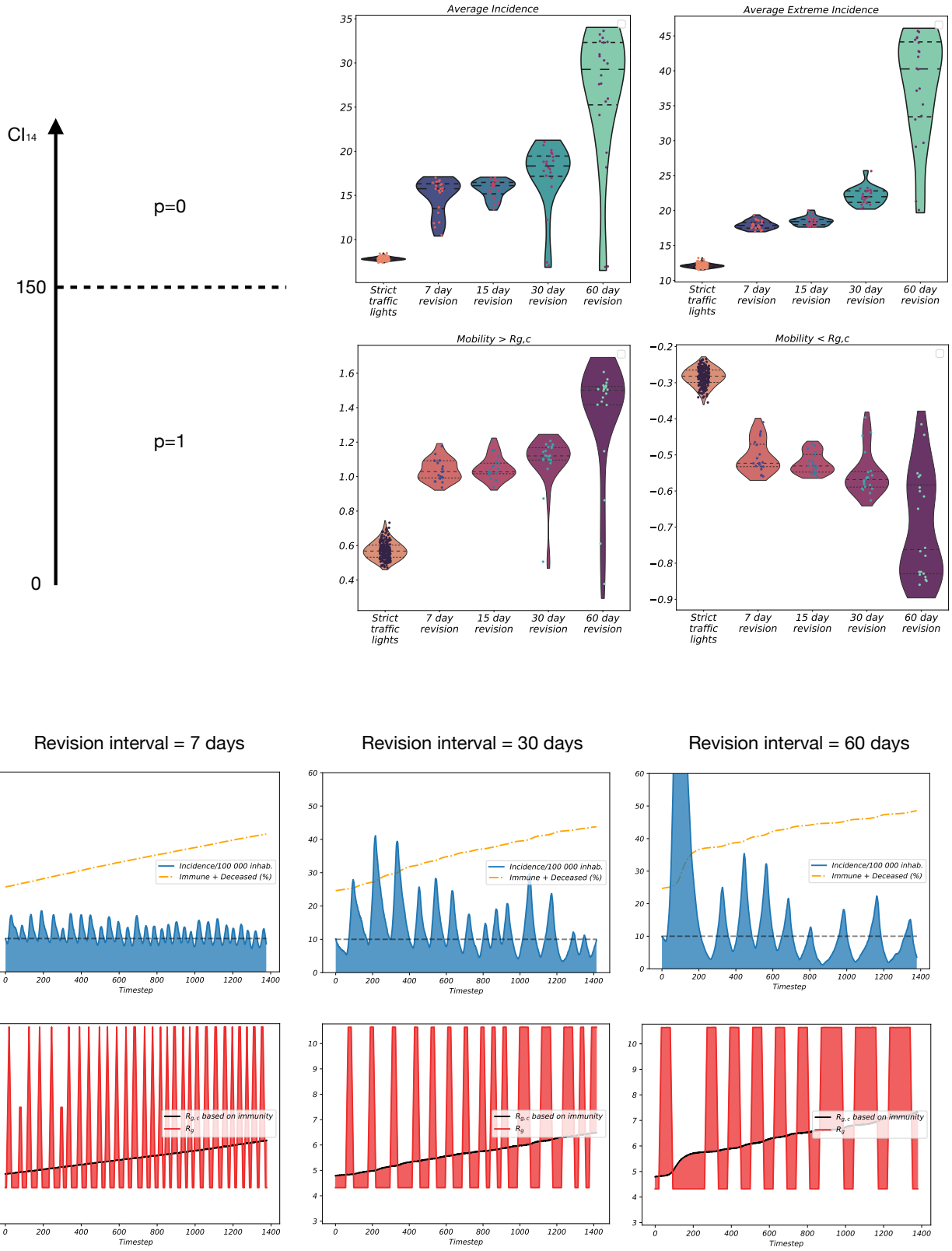

FIG. S10. Epidemic and mobility examples and statistics corresponding to the strict traffic light intervention described in the main text and a single threshold strict traffic light intervention with variable T_r.

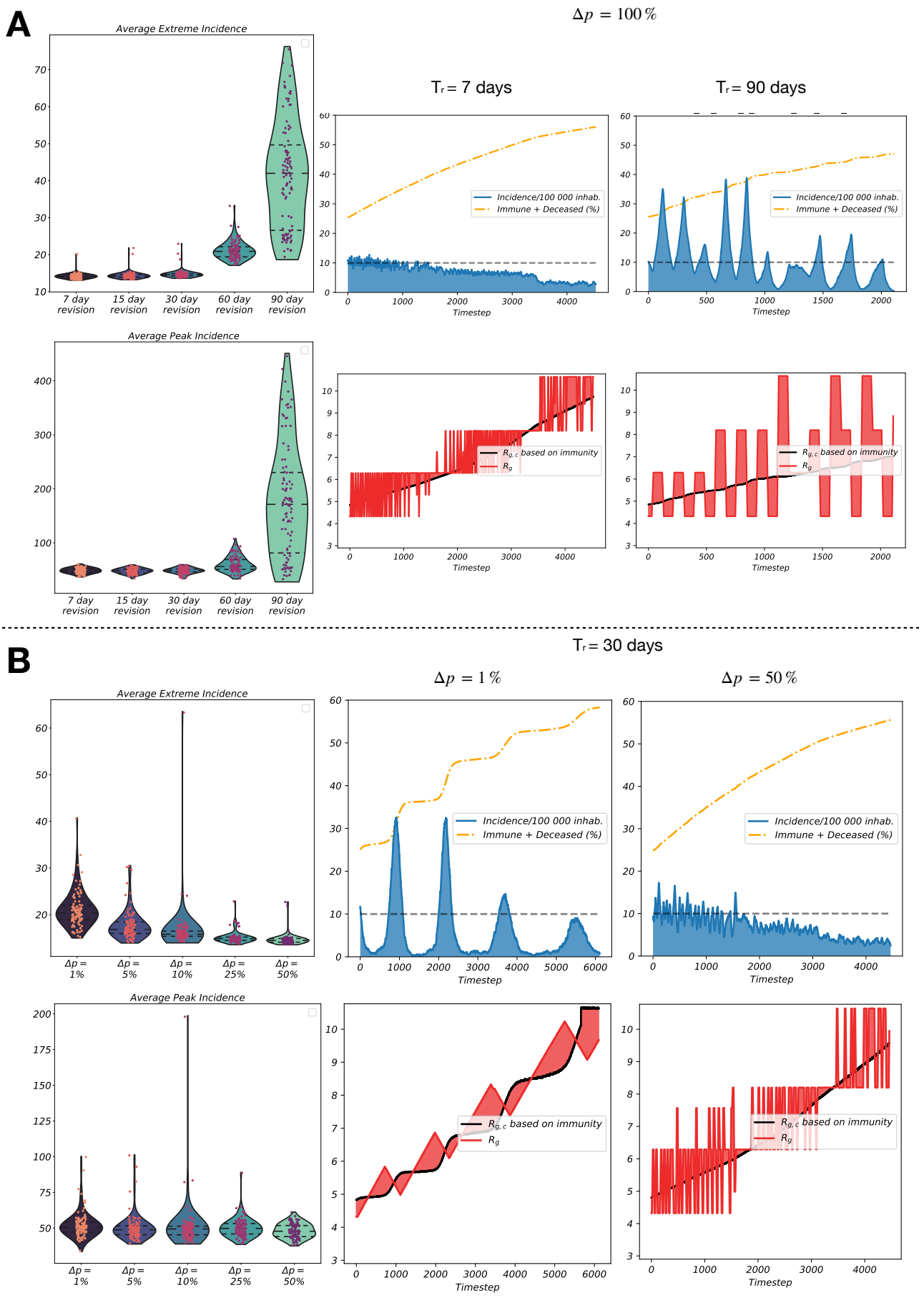

FIG. S11. A. Extreme incidence and peak incidence for a traffic light system with $\Delta p = 100\%$ and a variable revision interval T_r. B. Extreme incidence and peak incidence for a traffic light system with variable Δp and $T_r = 100$